Research Article | Vol. 14, No. 8 / 1 Aug 2023 / Biomedical Optics Express 4080
Biomedical Optics EXPRESS

Method to determine the centration of a lenticule of tissue extracted from a cornea

HAMED HAIDARI,[1,2] VICTOR DERHARTUNIAN,[3] AND SAMUEL ARBA-MOSQUERA[2,*]

[1]Technische Hochschule Aschaffenburg University of Applied Sciences (student), Aschaffenburg, D- 63743, Germany
[2]SCHWIND eye-tech-solutions, Kleinostheim, D- 63801, Germany
[3]EYELASER WIEN, Wien, D- 1010, Austria
[*]Samuel.Arba.Mosquera@eye-tech.net

Abstract: A simple and novel method to analyse the centration of a lenticule of tissue extracted from a cornea has been developed, in which the centre of "mass" of the individual differences between post and preoperative maps of several corneal metrics represents the lenticule centration and its spatial distance to a reference point (aimed centration) determines the decentration. Different parameters have been evaluated to weight the centre of "mass". The robustness of the methods has been evaluated using perturbation analysis (adding white-noise to the data) based on realistic uncertainties. A clipped analysis has been performed to prevent large, localised areas of lacking/missing data from affecting the centre of "mass". The method has been tested on a pilot cohort of clinical data showing 30% and 63% of the treatments within 200 µm of decentration for corneal thickness and refractive equivalent power, respectively. Except for anterior elevation with a total standard deviation of 17 µm, all other metrics show excellent precision of ~5 µm. The method provides a reliable and objective way to determine the centration of a lenticule of tissue extracted from a cornea and it can be applied to any topo- or tomographic derived metric.

1. Introduction

Corneal refractive surgery is a type of eye surgery that is used to correct vision problems by removing tissue from the cornea [1]. The cornea is the clear, dome-shaped surface of the eye that helps to focus light as it enters the eye. By removing tissue from the cornea, the shape of the cornea can be changed to improve vision.

One way to think about this tissue removal is by creating a lenticule with optical properties [2,3]. A lenticule is a small, lens-shaped piece of tissue that has been carefully cut out of the cornea to correct for refractive errors. For this treatment approach to be effective, it is important to centre the optical correction at a selected reference point, such as the corneal intersection of the visual axis. This ensures that the correction is applied in the correct location to improve vision [4].

However, if the actual correction is decentered with respect to this reference point, it can have a negative impact on visual performance. This can lead to problems such as coma (distorted vision), reduced contrast sensitivity, or reduced visual acuity [5]. Previous research has determined the permissible levels of decentration based on different optical measures [6]. Previous methods reported to determine lenticule centration often require operator input or involve subjective judgement [7]. This involves overlaying (manually/subjectively calibrated) circles and rulers over the image of a difference map to find the "best correspondence" between markers (circles and rulers) and the pseudo-colours in the difference map to determine (de-)centration (subjective judgement). This results in a fully manual, subjective, and time-consuming process.

The aim of this work is to develop and assess a new and simple method for analyzing the centration of a lenticule of tissue extracted from a cornea. This method would be operator

#495416 https://doi.org/10.1364/BOE.495416
Journal © 2023 Received 11 May 2023; revised 29 Jun 2023; accepted 30 Jun 2023; published 11 Jul 2023

Biomedical Optics EXPRESS

independent and unbiased and could be used to accurately assess the centration of the lenticule. In addition, this method may provide an alternative objective way to compare the accuracy and reproducibility to center a treatment on a specific target point at the cornea.

2. Methods

2.1. Difference between preoperative and postoperative measurements

The method to evaluate the centration of treatment is based on two topographic/tomographic measurements of the cornea (preoperative and postoperative). For each measurement, multiple metrics can be considered. Since the main mechanism of the corneal refractive surgery is to modify the curvature of the anterior surface of the cornea to modulate its optical power (in order to improve vision and visual quality without the use of any refractive aid (e.g. spectacles, contact lenses)), the metrics of interest for this work include corneal thickness (CT), anterior elevation (EA), corneal refractive equivalent power (REP), anterior refractive power (RFAP), and anterior sagittal (SA) and tangential curvatures (TAA) [8,9,10]. These metrics are typically available in the form of data matrices.

The method computes the difference between the postoperative and preoperative matrices for the selected metric (Fig. 1) and determines the centre of "mass" of the difference matrix. Of course, this is actually not the centre of mass in a rigorous manner. But the concept of centre of mass can be applied per analogy to corneal data. In a broader sense, the calculated centre is a "weighted average", but the centre of mass analogy provides a more intuitive interpretation.

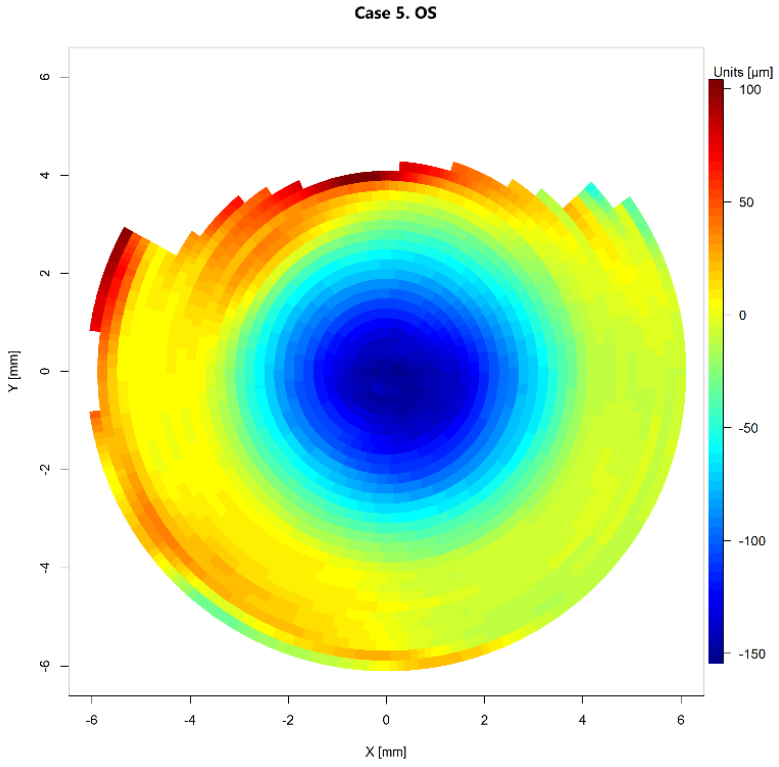

Fig. 1. Example of difference matrix (for the metric corneal thickness for case 5. of treatment OS) used to determine the centre of "mass"

Biomedical Optics EXPRESS

2.2. Centre of "mass"

The centre of mass refers to the point at which an object is perfectly balanced and would remain stable if it were supported at that point. The centre of mass is important because it determines how an object will behave when it is rotated or translated into space. For example, if the centre of mass of an object is not aligned with the point at which it is supported, the object may tip over or become unstable.

The centre of mass can be simply calculated for a collection of discrete points as:

$$X = \frac{\sum (x_i * w_i)}{\sum w_i} \tag{1}$$

$$Y = \frac{\sum (y_i * w_i)}{\sum w_i} \tag{2}$$

where X/Y are the coordinates of the centre of mass, x_i/y_i are the local coordinates within the data matrix, and w_i the weighting parameters (in the centre of mass analogy, the weightings would be the local mass of each individual data point).

2.3. Weighting parameters

In our method, the weighting parameters have been selected based on the initial inspection of the type of data (corresponding metric, i.e., measured signals). The measured signals are the values of the respective metric, i.e., using e.g., EA the elements in the matrices represent elevation data. We use these (elevation) data to determine the weights for the weighted average (analogy to centre of mass). For other metrics, we use the corresponding values in the matrices (what we call "the signals") to determine the weights for the weighted average.

Most of the metrics include positive and negative signals within the difference matrix (since we use the difference of the respective metric between pre- and post-surgery measurements, some matrix elements (of the difference matrices) may have positive values while other elements in the same matrix may have negative values). To account for the cancellation effects (the denominator of the weighted average (the sum of all weighting values for all matrix elements) becoming very small (or theoretically even zero)) and to prevent the denominator in the calculation of the centre of "mass" from approaching zero (leading to division by zero problem), each dataset has been shifted (either to be defined positively by subtracting the min value of the matrix from each of the values of the data points or to be defined negatively by subtracting the max value of the matrix from each of the values of the data points).

To provide flexibility, we have incorporated 2 parameters into the method. A global factor which scales the min/max value shift (i.e., a factor of zero would neglect the shift, a factor of unity would ensure a zero to peak signal distribution, and a factor of infinity (very large factors) would asymptotically approach a centroid calculation). The second parameter is an exponent (power) for the weightings (i.e., power of zero would correspond to a centroid calculation, power of unity would provide linear weightings, and power of 2 would base on quadratic weightings (thus also avoiding the cancellation effects of positive and negative signals within the difference matrix)).

The factor and power parameters are used to determine the weights for each value in the set of values. The factor parameter determines the relative weight of the min/max value in the set, while the power parameter determines the exponent to which the shifted value is raised. This corresponds to the following equations for the centre of "mass":

$$w_i = (Element_i - factor * Matrix_{min/max})^{\boldsymbol{power}} \tag{3}$$

where Element_i is the value of each element in the matrix (scanned through the index i), whereas $\text{Matrix}_{\text{min/max}}$ represents either the minimum or maximum value of the whole matrix.

The values for factor and power used in this work are presented in Table 1.

Biomedical Optics EXPRESS

Table 1. Weighting parameters for centre of "mass"

factor/power	0	1	2
0	0,0	0,1	0,2
1	1,0	1,1	1,2
2	2,0	2,1	2,2

2.4. Perturbation

To determine the robustness of the method and to account for the unavoidable uncertainties included in any single physical measurement, a perturbation analysis has been performed. [11,12]

Each matrix is modified (perturbed) with white-noise (perturbation) based on realistic uncertainties [13]. The appropriate values for the white-noise have been taken from previous reports [13], see Table 2.

Table 2. Noise based on realistic uncertainties taken from previous reports

Metrics	Noise
Corneal thickness	14 µm
Elevation anterior	10 µm
Refractive equivalent power	0.75 D
Refractive frontal power anterior	0.35 D
Sagittal anterior	0.35 D
Tangential anterior	0.75 D

Assuming gaussian error propagation, the perturbation of both pre and postoperative datasets independently can be simplified as a larger perturbation of the difference matrix.

$$Element_i = Element_i + (2{*}Random_i - 1){*}Noise{*}\sqrt{2} \tag{4}$$

where $Element_i$ (the value of each element in the difference matrix (scanned through the index i)) is perturbed with random noise ($Random_i$ for each element), Noise is the amplitude of the noise (as presented in Table 2), and the factor $\sqrt{2}$ corresponds to the effect of gaussian error propagation on two independent datasets (pre and postoperative). (2* $Random_i$ – 1) provides random values between -1 and +1, which are then scaled by the Noise amplitude times $\sqrt{2}$. Overall, in Eq. (4), $Element_i$ (the value of each element in the difference matrix (scanned through the index i)) is perturbed with random noise values (for each element) between -$\sqrt{2}$*Noise and +$\sqrt{2}$*Noise.

For the perturbation analysis, a loop is built for each case, 1 time without perturbation (ground truth) and n times with perturbation, which are then statistically analysed. The difference in the perturbed average centre of "mass" with respect to the ground truth corresponds to the accuracy of the method, whereas the standard deviation of the perturbed centre of "mass" represents the precision (reproducibility, robustness) of the method.

$$Totalstandarddeviation = \sqrt{\frac{\sum (\boldsymbol{standard\ deviation})^2}{\boldsymbol{n\ cases}}} \tag{5}$$

$$Totalerror = \frac{\boldsymbol{Totalstandarddeviation}}{\sqrt{\boldsymbol{n\ loops}}} \tag{6}$$

Biomedical Optics EXPRESS

2.5. Clipping

To prevent large, localized areas of lacking/missing data from affecting the centre of "mass", a clipping approach has been developed, in which the centre of "mass" is determined for subset data within a predetermined distance from the natural centre of the measurement (unlike the centre of "mass" based on all available points).

The center of the clipping diameter corresponds to the center of the tomographer data. Its physical position represents the corneal vertex normal (i.e., the most prominent point of the cornea, the point which is closer to the lens of the CCD camera of the videokeratoscope. At the vertex normal the cornea is also perpendicular to the videokeratoscope axis. On the acquired image, the vertex normal is the ideal center of the first (inner) mire).

The considered clipping radii are listed in Table 3

Table 3. Different radii for clipping

Radii	≤ 4.5 mm	≤ 4.0 mm	≤ 3.5 mm	≤ 3.0 mm	≤ 2.5 mm

For the clipped analysis, a loop is built for each case, 1 time for the whole dataset (potentially including regions with missing values) and n times with different clipping radii, which are then statistically analyzed. Both a difference in average clipped centre of "mass" respect to the whole dataset or a large standard deviation of the clipped centre of "mass" suggest that the difference matrix includes large, localized areas of lacking/missing data.

2.6. Clinical data for evaluation

The clinical data comes from treatments performed by a single surgeon (VD) in a single centre. The corneal measurements were performed with a Placido-Scheimpflug tomographer (SIRIUS, CSO, Italy) [14]. The treatments were performed using a lenticule extraction femtosecond laser system (SmartSight using SCHWIND ATOS, SCHWIND eye-tech-solutions, Germany). The dataset includes 101 eyes of 56 patients, 45 of them using bilateral data.

The used system provides the data matrices in polar/cylindrical coordinates based on constant radial and angular steps.

$$Azimuthal\ angle\ = 2\pi * \left(\frac{column\ index}{256}\right) \tag{7}$$

The equation obtains azimuthal angle from the column index. The column index goes from 0 to 255, with the azimuthal angle given in radians. The column indices were obtained from the pixel azimuthal position in a polar array of data. A full circle represents 2π radians. The first element (index zero) corresponds to 0 radians, the last element (index 255) corresponds to 2π*255/256 radians, since 2π radians are wrapped again to 0. The meridional step between columns corresponds to π/128 radians between equally azimuthally spaced meridians.

$$Radial\ distances = 6 * \left(\frac{row\ index}{30}\right) \tag{8}$$

The equation obtains radial distances from the row index. The row index goes from 0 to 30, with the radial distances given in mm. The row indices were obtained from the pixel radial position in a polar array of data. The full circle represents 6 mm radius. The first element (index zero) corresponds to 0 mm (origin of the data, which is redundant for all 256 azimuthal angles), the last element (index 30) corresponds to 6 mm. The radial step between rows corresponds to

Biomedical Optics EXPRESS

0.2 mm between equally radially spaced circles.

$$[x_{1,\ldots,i,\ldots,31*256}] = Radialdistances \ * \cos(Azimuthalangles) \tag{9}$$

$$[y_{1,\ldots,i,\ldots,31*256}] = Radialdistances * \sin(Azimuthalangles) \tag{10}$$

where all (31*256) combinations of radial distances and azimuthal angles are computed to determine x_i and y_i, which are then used in Eqs. (1) and 2 (via Eq. (3)) to determine the X and Y coordinate of the centre of "mass".

$$R = \sqrt{X^2 + Y^2} \tag{11}$$

$$\tan(\varphi) = \frac{Y}{X} \tag{12}$$

where R is the radial distance (the chord length) and φ the azimuthal angle (meridional axis) of the coordinate of the centre of "mass".

We have used polar matrices provided by the measurement device (a collection of points in a cylindrical coordinate system). The radial distances run from zero to 6 mm, thus the origin (centre of the maps) corresponds to the zero radial position, i.e. to the zero/zero cartesian position. The centre of the displayed maps is defined as the origin of the polar coordinate system corresponding to the center of the tomographer data. The centre of "mass" for each treatment and each metric has been determined (101 treatments * 6 metrics = 606 XY for the centre of "mass").

The 9 combinations, see Table 1, were computed twice (using both $Matrix_{min}$ and $Matrix_{max}$ to shift the weightings, leading to 18 combinations) for a specific Case to demonstrate how the calculations are performed.

The whole dataset has been evaluated using these parameters factor = 1, power = 1, including the following analyses:

- An XY plot for all metrics for both treatments (OD/OS) of a specific patient.
- XY plots for all treatments and two representative metrics (corneal thickness and refractive equivalent power) split in OD/OS.
- A statistical summary for every metric across all treatments (averages, standard deviations, minimum, and maximum, for each metric) and histograms for two representative metrics (corneal thickness and refractive equivalent power) across all treatments split in X, Y, R.
- Correlations between preoperative pupil offset and each metric.
- The differences in pupil center and limbus center positions (from pre- to post-operative) have been used as a sanity check.
- Correlations between the shift in limbus centre and each metric.

In the perturbation analysis, a loop of 6 iterations is performed for each case (treatment/eye), with the first iteration serving as the ground truth and 5 iterations involving perturbation. For these 5 perturbation iterations, the average and standard deviation of the centre of "mass" are calculated for each case. The average is used for the accuracy calculation and standard deviation for the robustness (reproducibility). The total standard deviation is calculated by taking the sum of the squares of the standard deviation of each case divided by 101 cases. The total standard error is calculated by dividing the total standard deviation by the square root of 5 iterations.

In the clipped analysis, a loop of 6 iterations is performed for each case (treatment/eye), with the first iteration using the whole matrix (potentially including regions with missing values) and 5 iterations involving decreasing radii. For these 5 clipped iterations, the average and standard deviation of the calculated centre of "mass" are determined for each case. Again, the total standard deviation is calculated by taking the sum of the squares of the standard deviation of each case divided by 101 cases. The total standard error is calculated by dividing the total standard deviation by the square root of 5 iterations.

Biomedical Optics EXPRESS

2.7. Technical implementation

The method has been implemented using the R - free software environment for statistical computing and graphics (https://www.r-project.org/). R is a language and environment for statistical computing and graphics. It is a GNU project which is similar to the S language and environment which was developed at Bell Laboratories (formerly AT&T, now Lucent Technologies) by John Chambers and colleagues. R can be considered as a different implementation of S. There are some important differences, but much code written for S runs unaltered under R. R provides a wide variety of statistical and graphical techniques and is highly extensible. The S language is often the vehicle of choice for research in statistical methodology, and R provides an Open-Source route to participation in that activity.

3. Results

3.1. Parameters

The 9*2 = 18 combinations, as Table 1 shows (using both $Matrix_{min}$ and $Matrix_{max}$ to shift the weightings), have been calculated for a specific Case and the results are shown in Table 4.

Table 4. Different weight combination for Case 5 OS and metric corneal thickness according to Eq. (3) using either $Matrix_{min}$ or $Matrix_{max}$ to shift the weightings

Min | Max	Power					
	0		**1**		**2**	
Factor	**Min**	**Max**	**Min**	**Max**	**Min**	**Max**
0	X: 0.051 mm Y: -0.404 mm R: 0.407 mm	X: 0.051 mm Y: -0.404 mm R: 0.407 mm	X: 0.361 mm Y: -0.223 mm R: 0.425 mm	X: 0.361 mm Y: -0.223 mm R: 0.425 mm	X: 0.099 mm Y: -0.091 mm R: 0.134 mm	X: 0.099 mm Y: -0.091 mm R: 0.134 mm
1	X: 0.051 mm Y: -0404 mm R: 0.407 mm	X: 0.051 mm Y: -0.404 mm R: 0.407 mm	X: -0.158 mm Y: -0.526 mm R: 0.549 mm	X: 0.168 mm Y: -0.336 mm R: 0.376 mm	X: -0.399 mm Y: -0.488 mm R: 0.631 mm	X: 0.190 mm Y: -0.252 mm R: 0.316 mm
2	X: 0.051 mm Y: -0404 mm R: 0.407 mm	X: 0.051 mm Y: -0.404 mm R: 0.407 mm	X: -0.027 mm Y: -0.450 mm R: 0.450 mm	X: 0.123 mm Y: -0.362 mm R: 0.383 mm	X: -0.127 mm Y: -0.474 mm R: 0.491 mm	X: 0.161 mm Y: -0.311 mm R: 0.350 mm

For the rest of the analysis, the whole dataset has been evaluated using factor = 1, power = 1, and $Matrix_{min}$ as parameters for Eq. (3).

The XY plot for Case 5 for all the metrics separated for OD and OS is presented in Fig. 2. The XY plot for corneal thickness and corneal refractive equivalent power for all cases is shown as Fig. 3. The summary for each metric across all treatments is presented in Table 5, and the corresponding histograms (for corneal thickness and corneal refractive equivalent power) of all treatments for X, Y, R in Fig. 4. Figure 5 displays the effects of clipping with different radii (as described in Table 3) for case 5 OS.

There was no significant correlation between preoperative pupil offset and any of the metrics. The results indicate that preoperative pupil offset does not affect the metrics, and that there is no relevant change in pupil offset from pre- to postoperative measurements. Additionally, the maximum deviation of differences in pupil centre and limbus centre positions was found to be

Biomedical Optics EXPRESS

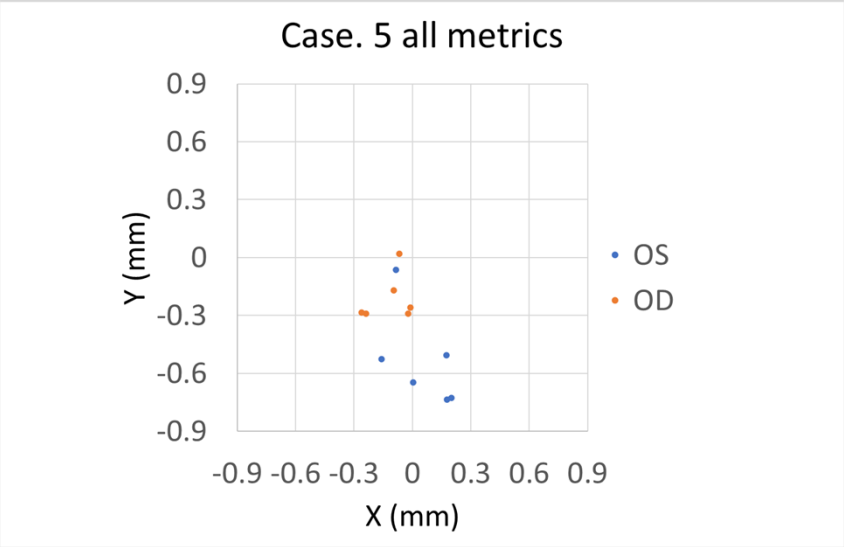

Fig. 2. Plot for all metrics (CT, EA, REP, RFPA, SA, TAA) of case 5. with treatment OS/OD

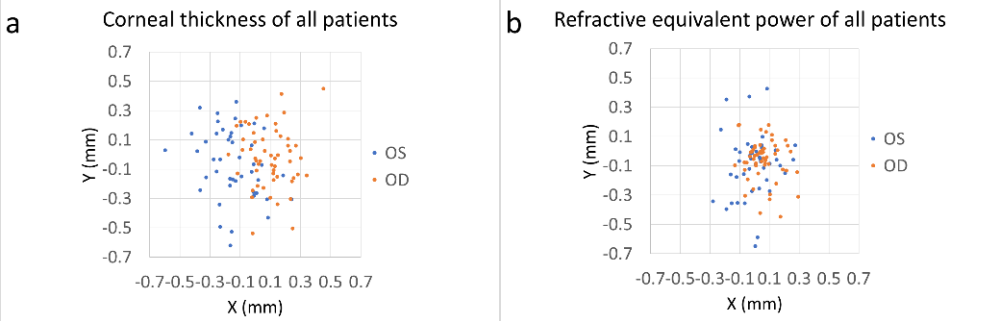

Fig. 3. X, Y plots for all treatments for the metrics a) corneal thickness. b) corneal refractive equivalent power

less than 200 µm. However, the centre of "mass" X coordinate correlated with the difference in the X coordinate of the limbus centre (respect to the corneal vertex normal) for 2 of the metrics (CT and TAA) ($p < .0001$ for both).

The accuracy of perturbation analysis is presented in Table 6. The total standard deviation and total standard error of the perturbation analysis are shown as Table 7.

Biomedical Optics EXPRESS

Table 5. Statistical summary of all treatments for all metrics of all the patients

		Mean	StdDev	Min	Max
corneal thickness (µm)	X	-5	207	-597	877
	Y	-27	232	-621	770
	R	270	157	26	905
anterior elevation (µm)	X	6	100	-217	287
	Y	-87	910	-256	246
	R	133	63	15	378
corneal refractive equivalent power (µm)	X	31	111	-280	294
	Y	-72	174	-647	428
	R	174	135	11	647
anterior refractive power (µm)	X	7	216	-576	536
	Y	-188	255	-764	629
	R	318	215	0	888
anterior sagittal (µm)	X	9	190	-408	426
	Y	-126	224	-727	607
	R	274	165	11	765
tangential curvatures (µm)	X	-21	125	-446	308
	Y	-63	218	-868	799
	R	206	158	23	878

Table 6. Accuracy (Difference in the perturbed average centre of "mass" with respect to the ground truth) of perturbation for all the treatments of all metrics for all patients

		Mean	**StdDev**	**Min**	**Max**
corneal thickness (µm)	X	1	20	-39	58
	Y	-1	21	-59	56
	R	24	16	0	67
anterior elevation (µm)	X	-4	60	-118	124
	Y	16	59	-168	111
	R	80	32	20	209
corneal refractive equivalent power (µm)	X	-1	9	-33	27
	Y	3	15	-57	51
	R	12	14	0	63
anterior refractive power (µm)	X	1	12	-33	24
	Y	8	17	-34	78
	R	16	15	0	81
anterior sagittal (µm)	X	0	13	-43	35
	Y	5	13	-28	35
	R	16	11	0	46
tangential curvatures (µm)	X	0	5	-12	17
	Y	0	7	-28	15
	R	5	5	0	28

Biomedical Optics EXPRESS

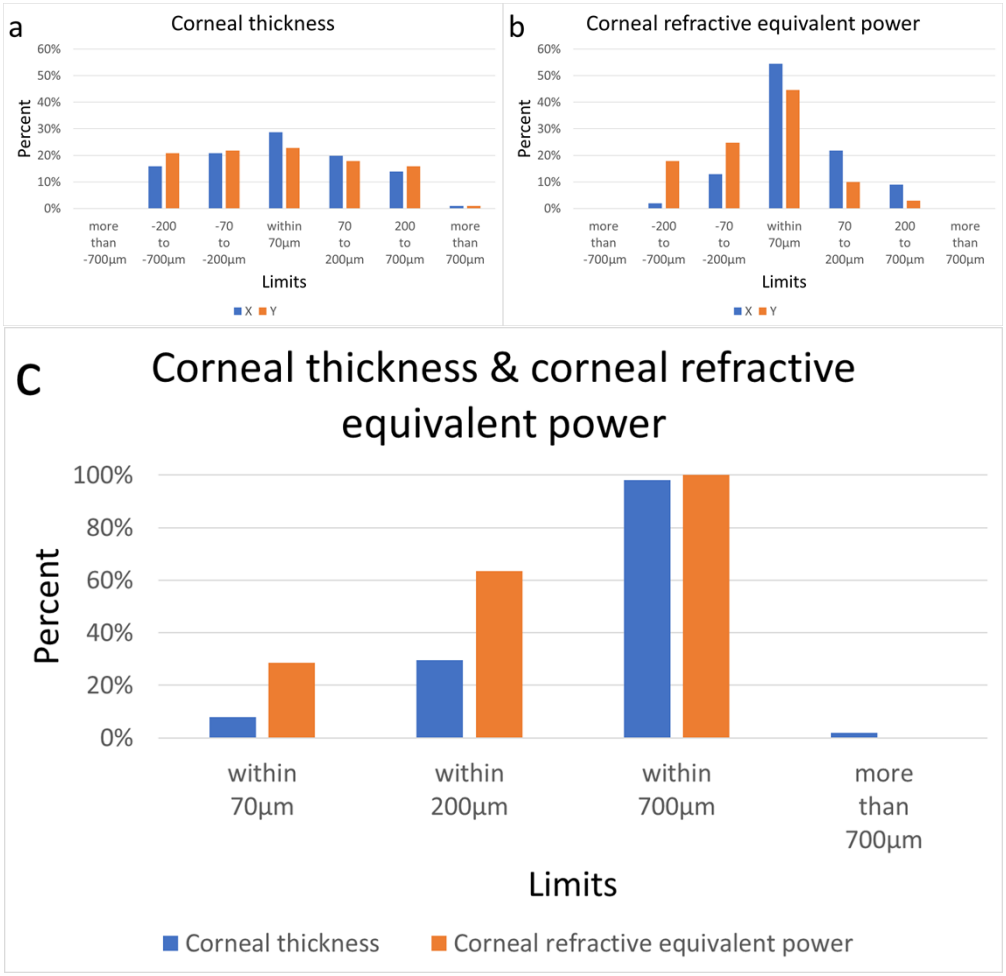

Fig. 4. distribution of X/Y for a) corneal thickness. b) corneal refractive equivalent power. c) distribution of R for corneal thickness and corneal refractive equivalent power.

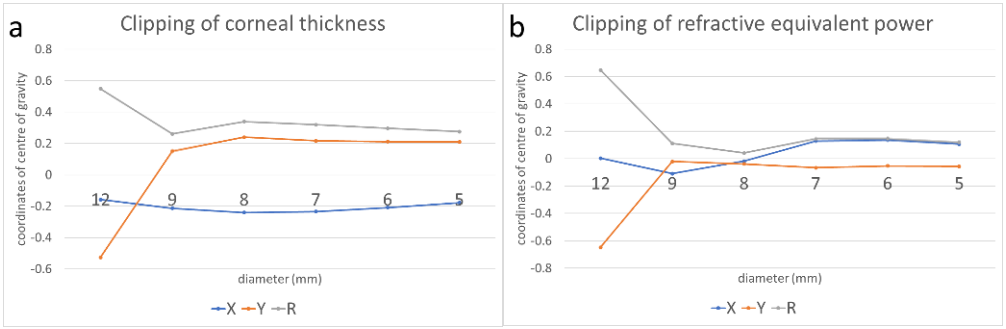

Fig. 5. Centre of "mass" for different clipping sizes (as described in Table 3) for case 5 OS. The X axis is simply labelled but not scaled, with the diameters in decreasing order. Due to missing values, clipping with different diameters shows a robust centre of "mass" for a) corneal thickness and b) corneal refractive equivalent power.

Biomedical Optics EXPRESS

Table 7. Total standard deviation and total error of perturbation

		Tot. StdDev	Tot. Err
corneal thickness (µm)	X	6	2
	Y	4	2
	R	6	2
anterior elevation (µm)	X	16	7
	Y	15	7
	R	16	7
corneal refractive equivalent power (µm)	X	5	2
	Y	6	2
	R	7	3
anterior refractive power (µm)	X	5	2
	Y	6	2
	R	7	3
anterior sagittal (µm)	X	4	2
	Y	4	2
	R	5	2
tangential curvatures (µm)	X	2	1
	Y	2	1
	R	3	1

4. Discussion

A method for determining the centration [15,16,17] of a lenticule of tissue extracted from a cornea has been successfully developed and evaluated. The method is simple and objective and its accuracy and reliability has been determined in a small pilot cohort. The method is universally applicable and can be used to analyse any metric that is susceptible to change from pre- to postoperatively [8,15,18].

The centration of the lenticule can be determined with respect to various references, such as the pupil centre, limbus centre, visual axis, or corneal vertex normal. The centre of the displayed maps is defined as the origin of the polar coordinate system and corresponds to the position of the corneal vertex normal.

The centre of mass is a point that is the average location of an object's mass distribution. It is the point where the object's mass distribution is balanced, so if the object were supported at this point, it would remain in equilibrium. The position of the centre of mass depends on the distribution of mass within the object. Therefore, the parameter sets (0,1), (0,2), (1,1), (1,2), (2,1), and (2,2) from Table 1 result in different centres of "mass" for the same difference matrix.

The centroid, on the other hand, is the geometric centre of an object (boundary contour). It is the average of all points in the object. The centroid is the point where the object's geometric axes intersect, such as the centre of a circle. The centroid is not affected by the actual mass distribution in the object and is only determined by the shape of the object. Therefore, the parameter sets (0,0), (1,0), and (2,0) from Table 1 (i.e., power = 0) determine the centroid of the difference matrices. For most cases, these two points (centroid and centre of "mass") are close to each other (as reported in Table 4), but conceptually they are not the same.

Both centroid and centre of "mass" calculations assume that the coordinates of the centre remain within the cloud of data. However, if there are missing data points or incomplete regions in the data, these methods can produce inaccurate or biased results. To address this issue, Hough algorithms can also be used to detect and compensate for missing data points, allowing for more

Biomedical Optics EXPRESS

accurate calculation of centroids and centres of "mass", even for complex shapes such as ellipses or weighted factors.

Since we use the difference of the respective metric between pre- and post-surgery measurements, the values may be positive or negative. Actually, some matrix elements (of the difference matrices) may have positive values while other elements in the same matrix may have negative values. This may make the denominator of the weighted average (the sum of all values for all matrix elements) very small (or theoretically even zero). We implicitly adopt the intuitive notion, that the centre (weighted average) of the lenticule/correction shall be restricted to the boundaries of the measured region. This can be ensured by preventing the denominator from becoming values close to zero (i.e., adding (or subtracting) a fixed term (factor*$\text{Matrix}_{\text{min/max}}$) to shift the weight for each element).

As mentioned for the parameter sets (0,1), (0,2), (1,1), (1,2), (2,1), and (2,2) from Table 1 we obtain the centre of "mass" of the difference matrices, but each set produces varying results. For example, using a factor of 0 and a power of 1 result in weights that are equal to the element itself (thus, they could even out), regardless of the minimum or maximum value in the set. On the other hand, using a factor of 0 and a power of 2 results in weights that are equal to the square of the element (thus, defined positive), regardless of the minimum or maximum value in the set. Using a factor of 1 and a power of 1, on the other hand, results in weights that are equal to the difference between the element and the extreme value in the matrix (which could be set to min or to max value of the matrix) and result in a zero to peak distribution of weightings. And accordingly for other values.

There is no intrinsic limitation for the factor and power to be integers between 0 and 2. They could have been any real values. We merely took the integers between 0 and 2 because they represent combinations which are easy/intuitive to interpret and relate to other methods. Non-integer values for the power, however, may lead to complex results (if the signals (i.e., Element_i) are negative).

A factor zero would neglect the shift, a factor one would ensure a zero to peak signal distribution, and a factor infinity (very large factors) would asymptotically approach a centroid calculation. An exponent (power) zero would correspond to a centroid calculation, a power of one would provide linear weightings, and a power of 2 would base on quadratic weightings.

In general, using a factor of 1 and a power of 1 will result in lower weights for elements that are closer to the extreme value, and higher weights for elements for that are farther from the extreme value. This can result in moderate variability in the weights. As reported in Table 4 the decentration for case 5 is stable at around 400 µm.

The method has been tested on a pilot cohort of clinical data and has been found to be effective. The different metrics provide complementary information about the geometry and optics of the lenticule. The X, Y plot of a specific metric for both treatments shows enantiomorphism [18,19] (mirror symmetry).

The (X, Y) given by different metrics are different but not very dissimilar. Actually, those (X, Y) coordinates closely match for obviously decentered cases (e.g., Case 5 OS). Figure 2 demonstrates differences in the decentration determined by several metrics. For OD, the Y component of the decentration given by different metrics ranges from about +20 µm (EA) to -290 µm (RFPA), whereas for OS, it ranges from -60 µm (EA) to -730 µm (RFPA). If we exclude EA from the Figure, the other 5 metrics agree within 100 µm standard deviation for X and Y for both OD and OS.

The primary aim of this work is neither determining the optimum centration reference for clinical use, nor finding the most adequate metric to evaluate centration. Rather, the aim of the work is to present a simple yet novel method to assess centration in an objective way without any subjective or manual step. When a new method is presented, it is usually needed to prove that the results given by the method are reliable, or they agree with the experimental results. The

Biomedical Optics EXPRESS

best way is to provide experimental results to show which metric gives the best estimation of the centration. Explaining why in some cases, there are large differences in the (X,Y) given by different methods may point out which metric should be used to evaluate the centration and why.

The discussion on different metrics to evaluate centration has been subject to debate in clinical papers, as it can be seen in the references. In particular, Chung et al. [7] and Roberts [20] have provided discussion on the topic.

Which of the provided metrics is more reliable may depend on several factors. On the one hand, one can check at the perturbation analysis which metric is more robust (i.e., less prone to be affected by noise) and take this as the best representing the unbiased centration (i.e., TAA). On the other hand, one can split the presented metrics into 2 general groups: metrics representing length data (CT and EA) and metrics representing curvature/power data (the rest) (actually one could further split this into curvature vs power data, although both are typically presented in dioptres). With this split, one could say that for evaluating the centration of the lenticule as "a volume of tissue" metrics representing length data seem more adequate (and of those take the one with the lowest perturbation, i.e., CT), whereas for evaluating the refractive effect of the correction metrics representing curvature/power data seem more adequate (and of those take the one with the lowest perturbation, i.e. TAA).

It is difficult to discuss the accuracy of the centration partly due to the lack of an absolute optimum centration reference. Concerning the optimum centration reference, previous work has discussed and presented the currently available different approaches [4]. Concerning the question regarding the accuracy of the method, this can be determined using idealised synthetic files (instead of pre- and postoperative data of real treatments). By doing this (unpublished data), the model properly retrieves the virtually applied decentration. Another limitation of the true performance of the model is the actual resolution of the diagnostic data (200 µm radially in our case).

Comparing both panels of Fig. 3 also suggests differences between the decentration determined using either CT or REP. Analyzing those differences reveals centred differences with a close to zero average and ~150 µm µm standard deviation for X and Y, with 75% of the cases showing differences within 200 µm for X and Y. Furthermore, there is a statistically significant correlation ($p < .0001$) between the decentration determined using CT and REP for both X and Y components of the determined decentration, suggesting that the determined decentrations correspond to a true shift of the centre of "mass" of the dataset of the differences.

Histograms showing the distribution of decentrations have been generated based on different optical metrics [21–26]. The method has been compared to other methods for determining centration/decentration of corneal corrections, most of which require operator input or subjective judgement [7,21,22]. The evaluation of our pilot cohort (101 cases) shows that decentration remains within 200 µm in 30% of the cases for CT and 63% of the cases and REP (Fig. 4(c)).

A formal reproducibility analysis has been performed based on the perturbation analysis. We believe that the uncertainties in the method determined by the perturbation analysis properly represent the reproducibility when using multiple pre-op and multiple post-op measurements. Adding noise to the dataset means introducing random variation or uncertainties to the location of the centre of "mass". This can be done, for a variety of reasons, such as to simulate real-world conditions or to test the robustness of the lenticule decentration. This can help to identify potential weaknesses and make necessary adjustments. In general, a perturbation analysis involves making small changes to a system and observing the effects on that system. This can be used to assess the accuracy and robustness of a method. The perturbation analysis involves comparing the average centre of "mass" with and without small changes, or perturbation, to the system. The difference between the two represents the accuracy of the method as reported in Table 6, and the standard deviation of the perturbed centre of "mass" represents its robustness [11,12].

Biomedical Optics EXPRESS

One could perform the perturbation analysis based on a real series of different measurements of the cornea (pre and post) instead of based on a white-noise approach, yet this would add other sources of confounding factors beyond the robustness of the method itself. Alternatively, one could perform the perturbation analysis merely based on the perturbation of the elevation data and take these then to formally calculate all the other metrics. The selected approach is simpler than that one, since it does not involve any reconstruction, but it is equivalent since the noise amplitudes have been selected based on realistic modelling. Finally, the selected approach in which every metric is perturbed "on its own" and in a sense independently, may provide a larger coverage of the perturbation applied to these 101 cases.

Total standard deviation and total standard error are measures of the variability or dispersion of a set of data. A lower total standard deviation and total standard error indicate that the dataset is more reproducible, which indicates that the method is more reliable. Additionally, it makes it easier to detect small but significant differences. Except for EA with a total standard deviation of less than 17 µm, all the other metrics have excellent precision and robustness of ~5 µm overall (Table 7).

Adding 10 µm noise to EA data causes that the (z) value of the pre- to postoperative difference for each element (pixel) changes within ± 14 µm. The actual effect caused by the noise is more important (more detrimental) in the centre of EA (for which the sagittal elevation z values for neighbour elements are close to each other, with radial slopes <0.05 (50 µm/mm), approx. ~1 mm diameter centrally) and reduced in the periphery (for which the sagittal elevation z values for neighbour elements are farther apart, becoming negligible approx. from 8 mm diameter to the outside).

The results indicate that preoperative pupil offset does not affect the metrics, and that there is no relevant change in pupil offset from pre- to postoperative measurements. Additionally, the maximum deviation of differences in pupil centre and limbus centre positions was found to be less than 200 µm (within the radial resolution of the data matrices). The reference point that could be derived from a Placido-Scheimpflug measurement, such as the corneal intersection of the visual axis, is actually subject to be dependent on the optics and geometry of the cornea. So, comparing pre- and post-operative data might be biased by a change of the visual axis that occurred through the optical correction itself. Since both, pupil and limbus centres, did not change location (respect to the centre of the map, the corneal vertex normal) from pre- to postoperative measurements, we can infer that the centre of the map, i.e., the corneal vertex normal, remained largely unchanged by the treatment.

Since the centre of "mass" X coordinate correlated with the difference in the X coordinate of the limbus centre (respect to the corneal vertex normal) for 2 of the metrics (CT and TAA, $p < .0001$ for both), we repeated the analyses considering the decentration respect to the position of the preoperative corneal vertex normal (i.e., accounting for the shifts in limbus centre respect to the corneal vertex normal). While the numbers vary, the distribution of the decentration remained the same. This is shown in Fig. 6.

From Tables 6 and 7 combining the accuracy and the variance of the perturbation analysis, it can be inferred that this method would be reproducible (95% limits of agreement) to at least 53 µm (CT), 148 µm (EA, see the discussion above), 38 µm (REP), 44 µm (RFPA), 36 µm (SA), and 16 µm (TAA). All of these but EA are below the relevant tolerance of 70 µm to achieve the diffraction limit in 95% of the normal eyes with a 7.0 mm pupil, and EA is well within the 200 µm tolerance to reach the same goal with a 3.0 mm pupil [6].

The intention of clipping is to determine the center of "mass" based only on the subset of the matrix that fulfills a certain radius criterion. This means that the center of "mass" will be calculated using only the elements of the matrix that are within a certain distance of some reference point, in our case the corneal vertex normal (Table 3), and any elements that are outside of this distance are ignored. One reason to do this is to ensure that the center of "mass" is

Biomedical Optics EXPRESS

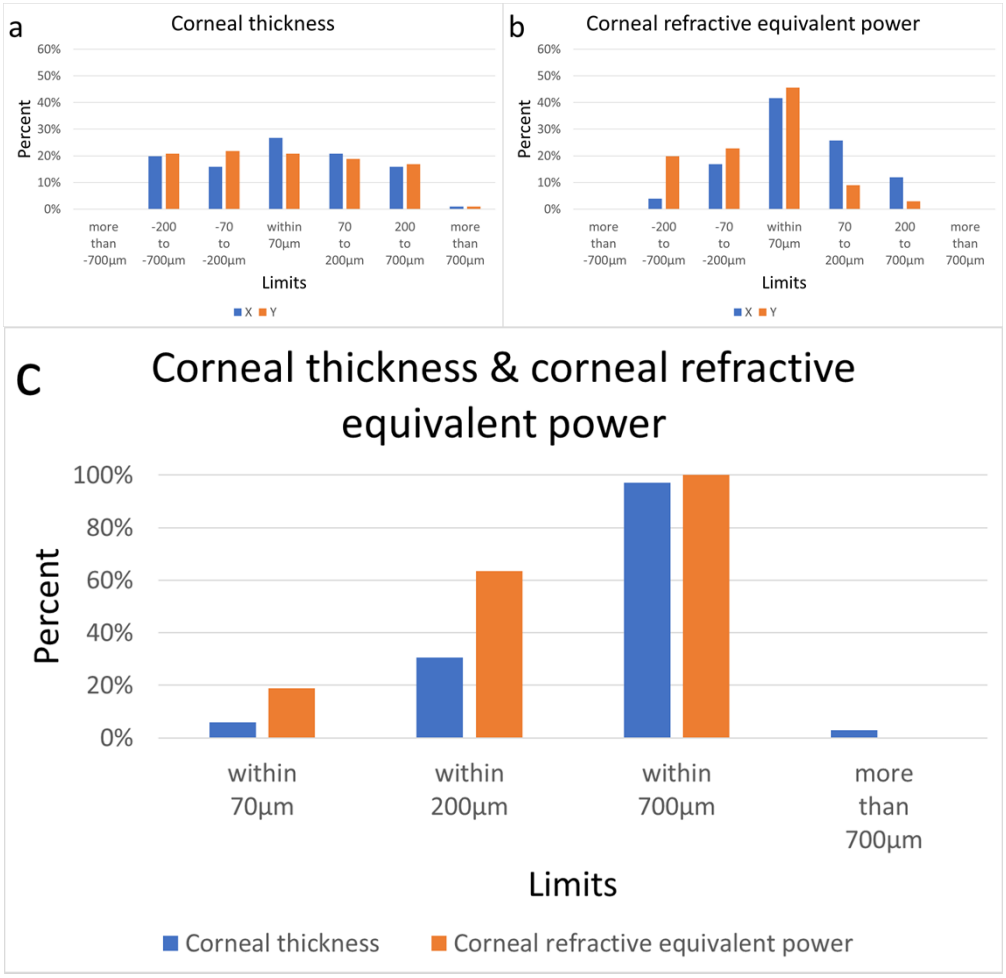

Fig. 6. Frequency of decentration respect to the position of the preoperative corneal vertex normal (i.e., accounting for the shifts in limbus centre respect to the corneal vertex normal). Distribution of X/Y for a) corneal thickness. b) corneal refractive equivalent power. c) distribution of R for corneal thickness and corneal refractive equivalent power.

calculated using a consistent set of points, rather than being influenced by extreme, outlying, or missing values. By clipping the matrix and only considering a subset of its elements, values that might skew the result are ignored and provide a better estimate of the center of "mass". This information can be useful for improving the accuracy and robustness of the dataset and method and enables the detection of inconsistent diagnostic data.

A strong clipping criterion, in which a very small subset of the matrix is used to calculate the center of "mass", could falsely reduce the estimated decentration. This is because the clipping process effectively ignores large portions of the matrix, which could include important information about the distribution of the data. As a result, the center of "mass" calculated using a strongly clipped matrix may not accurately reflect the true distribution of the data and could underestimate the decentration.

In general, it is important to carefully consider the clipping criterion used in any analysis. If the criterion is too strong, it could lead to inaccurate or unreliable results, while if the criterion is too weak, it may not effectively filter out extreme or outlying values. It is therefore important to

Biomedical Optics EXPRESS

strike a balance between using a sufficiently restrictive criterion to exclude unreliable data, while still including enough data to accurately represent the true distribution of the data.

The centre of "mass" of Case 5 is stable for any of the suggested clipped diameters (<= 9 mm, >=5 mm) and corresponds to the missing data observable at Fig. 1, but also to the values observed at Table 4 and Fig. 2. Differences in pupil centre and limbus centre positions before and after surgery were used as a sanity check to ensure that the measurements are well aligned and do not introduce confounding effects. Overall, the method provides a reliable and objective way to determine the centration of a lenticule of tissue extracted from a cornea. Theoretically, the same method can be easily used on pre- or post-surgery data to determine the most appropriate centration for a spectacle-like correction (sphere, cylinder, and axis), proxy for the visual axis [27].

The centre provided by the current method (based on pre to post surgery differences) represents the effective centration of the applied correction; whereas comparing the centres determined based on isolated pre- and post-surgery data represents a potential shift of the visual axis induced by the surgery [27].

5. Conclusions

A new method has been developed for analyzing the centration of a lenticule of tissue extracted from the cornea. This simple method has been evaluated in a small cohort, providing an objective and less error-prone approach to lenticule centration analysis.

This method is non-invasive, operator-independent, and generic, making it a valuable tool in ophthalmic surgery and research. It enables reliable and accurate measurement of corneal refractive surgery procedures and can be applied to any topo- or tomographic derived metric.

The evaluation of this new approach has demonstrated its validity and the accuracy of the centration values. Overall, the method could be helpful to support further improvements in corneal laser surgery and would allow surgeons to assess the quality of their outcomes as well as to assess different products in the market regarding their reliability in centration.

Acknowledgments. The article has not been presented at any meeting. The authors did not receive any financial support from any public or private sources. The authors have no financial or proprietary interest in a product, method, or material described herein. The article represents the personal views of the authors and was not written as a work for hire within the terms of the author's employment. The work described in the article itself (as opposed to the work done writing the article) was conducted as part of the author's work. Content attributed to the authors was vetted by a standard approval process for third-party publications.

Disclosures. Samuel Arba-Mosquera and Hamed Haidari are employees of SCHWIND eye-tech-solutions, manufacturer of the SCHWIND ATOS femtosecond system for refractive surgery.

Data availability. Data underlying the results presented in this work are not publicly available at this time but may be obtained from the authors upon reasonable request.

References

1. C. R. Munnerlyn, S. J. Koons, and J. Marshall, "Photorefractive keratectomy: a technique for laser refractive surgery," J Cataract Refract Surg. **14**(1), 46–52 (1988).
2. W Sekundo, K Kunert, C Russmann, A Gille, W Bissmann, G Stobrawa, M Sticker, M Bischoff, and M. Blum, "First efficacy and safety study of femtosecond lenticule extraction for the correction of myopia: six-month results. J Cataract Refract Surg," Erratum in: J Cataract Refract Surg. **34**(9), 1513–1520 (2008).
3. M. Blum and W. Sekundo, "Femtosekunden-Lentikel-Extraktion (FLEx) [Femtosecond lenticule extraction (FLEx)]," Ophthalmologe. **107**(10), 967–970 (2010).
4. Arba Mosquera S, S Verma, and C. McAlinden, "Centration axis in refractive surgery," Eye Vis (Lond). **2**(1), 4 (2015).
5. M. Mrochen, M. Kaemmerer, P. Mierdel, and T. Seiler, "Increased higher-order optical aberrations after laser refractive surgery: a problem of subclinical decentration," J Cataract Refract Surg. **27**(3), 362–369 (2001).
6. M. Bueeler, M. Mrochen, and T. Seiler, "Maximum permissible lateral decentration in aberration-sensing and wavefront-guided corneal ablation," J Cataract Refract Surg. **29**(2), 257–263 (2003).
7. B. Chung, H. Lee, C. J. Roberts, D. S. Y. Kang, D. Z. Reinstein, S. K. Jean, E. K. Kim, K. Y. Seo, and T. I. Kim, "Decentration measurements using Placido corneal tangential curvature topography and Scheimpflug tomography

Biomedical Optics EXPRESS

pachymetry difference maps after small-incision lenticule extraction," J Cataract Refract Surg. **45**(8), 1067–1073 (2019).
8. M. C. Arbelaez, C. Vidal, and S. Arba Mosquera, "Central Ablation Depth and Postoperative Refraction in Excimer Laser Myopic Correction Measured With Ultrasound, Scheimpflug, and Optical Coherence Pachymetry," J Refract Surg **25**(8), 699–708 (2009).
9. A. Mosquera S and I. M. Aslanides, "Analysis of the effects of Eye-Tracker performance on the pulse positioning errors during refractive surgery," J Optom. **5**(1), 31–37 (2012).
10. A. Mosquera S and T. Ewering, "New asymmetric centration strategy combining pupil and corneal vertex information for ablation procedures in refractive surgery: theoretical background," J. Refract. Surg. **28**(8), 567–575 (2012).
11. A. Mosquera S and S. Verma, "Numerical nonwavefront-guided algorithm for expansion or recentration of the optical zone," J. Biomed. Opt **19**(8), 088001 (2014).
12. S. Verma, J. Hesser, and S. Arba-Mosquera, "Optimum Laser Beam Characteristics for Achieving Smoother Ablations in Laser Vision Correction," Invest. Ophthalmol. Vis. Sci. **58**(4), 2021–2037 (2017).
13. Alfonso Pérez-Escudero, Carlos Dorronsoro, and Susana. Marcos, "Correlation between radius and asphericity in surfaces fitted by conics," J. Opt. Soc. Am. A **27**(7), 1541–1544 (2010).
14. G. Savini, P. Barboni, M. Carbonelli, and K. J. Hoffer, "Repeatability of automatic measurements by a new Scheimpflug camera combined with Placido topography," J Cataract Refract Surg. **37**(10), 1809 (2011).
15. M. Camellin and S. Arba Mosquera, "Aspheric Optical Zones: The Effective Optical Zone with the SCHWIND AMARIS," J. Refract. Surg. **27**(2), 135 (2011).
16. M. Camellin and S. Arba Mosquera, "Aspheric Optical Zones in hyperopia with the SCHWIND AMARIS," J Optom. **4**(3), 85–94 (2011).
17. M. C. Arbelaez, C. Vidal, and S. Arba Mosquera, "Clinical outcomes of corneal vertex versus central pupil references with aberration-free ablation strategies and LASIK," Invest. Ophthalmol. Vis. Sci. **49**(12), 5287 (2008).
18. M. C. Arbelaez, C. Vidal, and S. Arba-Mosquera, "Bilateral Symmetry before and Six Months after Aberration-Free™ Correction with the SCHWIND AMARIS TotalTech Laser: Clinical Outcomes," J Optom **3**(1), 20–28 (2010).
19. A. Mosquera S and S. Verma, "Bilateral symmetry in vision and influence of ocular surgical procedures on binocular vision: A topical review," J Optom. **9**(4), 219–230 (2016).
20. C. J. Roberts, "Error in the estimation of ablation centration using pachymetric difference maps," J. Refract. Surg. **31**(2), 138–139 (2015).
21. H. Lee, C. J. Roberts, S. Arba-Mosquera, D. S. Y. Kang, D. Z. Reinstein, and T. I. Kim, "Relationship Between Decentration and Induced Corneal Higher-Order Aberrations Following Small-Incision Lenticule Extraction Procedure," Invest. Ophthalmol. Vis. Sci. **59**(6), 2316–2324 (2018).
22. D. S. Y. Kang, H. Lee, D. Z. Reinstein, C. J. Roberts, S. Arba-Mosquera, T. J. Archer, E. K. Kim, K. Y. Seo, and T. I. Kim, "Comparison of the Distribution of Lenticule Decentration Following SMILE by Subjective Patient Fixation or Triple Marking Centration," Journal of Refractive Surgery **34**(7), 446–452 (2018).
23. I Jun, DSY Kang, DZ Reinstein, S Arba-Mosquera, TJ Archer, KY Seo, and TI. Kim, "Clinical Outcomes of SMILE With a Triple Centration Technique and Corneal Wavefront-Guided Transepithelial PRK in High Astigmatism," J. Refract. Surg. **34**(3), 156–163 (2018).
24. Arba Mosquera S and S. Verma, "A review of clinical outcomes following SMILE for the treatment of astigmatism," Expert Rev. Ophthalmol. **15**(6), 321–330 (2020).
25. S. Arba-Mosquera, S. Verma, and S. T. Awwad, "Theoretical Effect of Coma and Spherical Aberrations Translation on Refractive Error and Higher Order Aberrations," Photonics **7**(4), 116 (2020).
26. S. A. Mosquera and D. de Ortueta, "Theoretical influence of decentred ablations on induced coma aberrations," J. Emmetropia **2**, 153–158 (2011).
27. S. A. Mosquera, D. de Ortueta, and S. Verma, "Corneal functional optical zone under monocular and binocular assessment," Eye and Vision **5**, 3 (2018).